

# Reversible and Irreversible Chemisorption in Nonporous-Crystalline Hybrids\*\*

Diego Solis-Ibarra and Hemamala I. Karunadasa\*

**Abstract:** The tools of synthetic chemistry allow us to fine-tune the reactivity of molecules at a level of precision not yet accessible with inorganic solids. We have investigated hybrids that couple molecules to the superior thermal and mechanical properties of solids. Herein we present, to the best of our knowledge, the first demonstration of reactivity between hybrid perovskites and substrates. Reaction with iodine vapor results in a remarkable expansion of these materials (up to 36% in volume) where new covalent C–I bonds are formed with retention of crystallinity. These hybrids also show unusual examples of reversible chemisorption. Here, solid-state interactions extend the lifetime of molecules that cannot be isolated in solution. We have tuned the half-lives of the iodinated structures from 3 h to 3 days. These nonporous hybrids drive substrate capture and controlled release through chemical reactivity. We illustrate the strengths of the hybrid by considering radioactive iodine capture.

The vast majority of materials designed for gas capture features cavities matched in size with the guest molecules, pores with substrate-binding sites or flexible pore walls.<sup>[1]</sup> Nonporous materials have not been widely investigated for storage applications owing to the obvious lack of void space. There are, however, a few examples of nonporous coordination polymers<sup>[2]</sup> and organic-molecular crystals<sup>[3]</sup> that can store volatile molecules. Hybrid perovskites allow for the incorporation of organic and inorganic components in a single-phase and well-defined structure via solution-state self-assembly.<sup>[4]</sup> They consist of two-dimensional anionic coordination polymers comprised of corner-sharing metal-halide octahedra alternating with ordered arrays of organic cations. These materials form close-packed structures and we are not aware of any reports of reactions that occur between hybrid perovskites and substrates. A reversible volume expansion upon solvent intercalation has been reported in

these layered structures,<sup>[5]</sup> and we investigated if this could be extended to inducing reactivity in the organic layers of the hybrid.

Solution-state reactions of elemental iodine with terminal alkynes and alkenes to form diiodoalkenes and diiodoalkanes, respectively, are well known.<sup>[6]</sup> Therefore, we started our studies with a family of hybrids featuring alkyne/alkene groups in the organic layers (Figure 1). Alkyne–ammonium

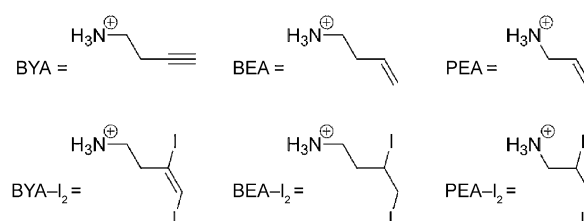


Figure 1. Structures of the organic cations used.

groups in the hybrid perovskite (BYA)<sub>2</sub>[PbBr<sub>4</sub>] (**1**) form a close-packed, partially interdigitated bilayer (Figure 2a);<sup>[7]</sup> a probe radius of 0.8 Å shows a solvent-accessible volume of only 1.2 Å<sup>3</sup>, or 0.1% of the unit cell.<sup>[8]</sup> However, exposure of this solid to iodine vapor results in a dramatic expansion of the spacing between the inorganic sheets as iodine is incorporated into the organic layers through the irreversible formation of BYA–I<sub>2</sub> molecules. Upon iodination of single crystals of **1** we repeatedly obtained crystals that allowed us to determine unit-cell parameters using single-crystal X-ray diffraction, although they were not of sufficient quality to solve the full structure. This is likely due to the strain resulting from the massive unit-cell expansion. We therefore recrystallized the product and obtained well-formed single crystals for structure determination.<sup>[7]</sup> The simulated powder pattern from the crystal structure matches the powder diffraction pattern of the crude iodination-reaction product, confirming that the same material is formed in both cases (Supporting Information, Figure S3). This reaction proceeds through a topotactic transformation<sup>[9]</sup> that preserves the layered structure. The inorganic template maintained in the crystalline product restricts expansion in the direction of the crystallographic *a* and *b* axes and the unit cell expands almost exclusively in the direction of the crystallographic *c* axis (corresponding to the distance between inorganic sheets). Remarkably, the *c* axis expands by 38% and the unit-cell volume increases by 36% compared to the parent structure (Table 1), while retaining a high degree of crystallinity. The (BYA–I<sub>2</sub>)<sub>2</sub>[PbBr<sub>4</sub>] perovskite (**1-2 I<sub>2</sub>**; Figure 2b) affords a gravimetric capacity of 43 wt % (0.43 g of I<sub>2</sub> per 1 g

[\*] Dr. D. Solis-Ibarra, Prof. H. I. Karunadasa  
Department of Chemistry, Stanford University  
Stanford, CA 94305 (USA)  
E-mail: hemamala@stanford.edu  
Homepage: <http://www.stanford.edu/group/karunadasalab/>

[\*\*] This research was funded by the Precourt Institute for Energy and the Stinehart/Reed Awards Fund. We thank Stanford University for generous start-up funds and the Stanford Gabilan Fund for partial support of D.S. Single-crystal and powder X-ray diffraction studies were performed at the Stanford Nanocharacterization Laboratory (SNL), part of the Stanford Nano Shared Facilities. We also thank M. Gembicky for assistance with crystallography, and Profs. J. Du Bois, R. M. Waymouth, and J. I. Brauman for helpful discussions.

Supporting information for this article is available on the WWW under <http://dx.doi.org/10.1002/anie.201309786>.

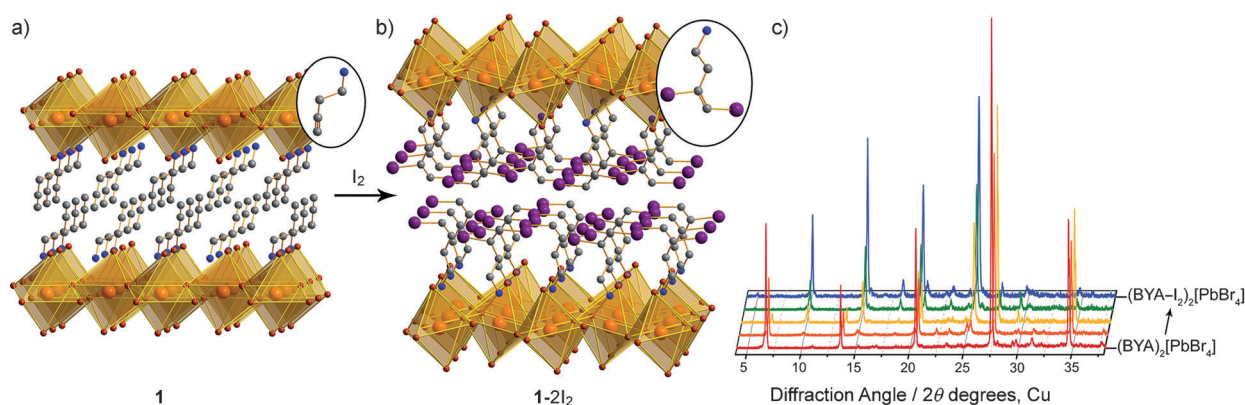


**Figure 2.** X-ray structures of a)  $(\text{BYA})_2[\text{PbBr}_4]$  (**1**) and b) its reaction product with iodine:  $(\text{BYA-I}_2)_2[\text{PbBr}_4]$  (**1-2I<sub>2</sub>**). Insets show the cations in the organic layers. H atoms omitted for clarity. Pb orange, I purple, Br brown, N blue, C gray. c) Powder X-ray diffraction patterns of an oriented film of **1** after various exposure times to iodine vapor, showing conversion into **1-2I<sub>2</sub>**.

**Table 1:** Unit-cell parameters for  $(\text{BYA})_2[\text{PbBr}_4]$  and  $(\text{BYA-I}_2)_2[\text{PbBr}_4]$ .

	$(\text{BYA})_2[\text{PbBr}_4]$ ( <b>1</b> )	$(\text{BYA-I}_2)_2[\text{PbBr}_4]$ ( <b>1-2I<sub>2</sub></b> )	Difference
space group	$P2_1/c$	$P\bar{1}$	
<i>a</i> [Å]	7.819(1)	7.982(1)	0.163
<i>b</i> [Å]	8.396(1)	8.142(1)	−0.254
<i>c</i> [Å]	12.808(1)	17.630(1)	<b>4.822</b>
α [°]	90	88.425(2)	−1.575
β [°]	93.504(2)	85.355(2)	−1.141 <sup>[a]</sup>
γ [°]	90	89.868(2)	−0.132
volume [Å <sup>3</sup> ]	838.2(1)	1141.6(2)	<b>303.4</b>

[a] The supplementary angle of  $(\text{BYA})_2[\text{PbBr}_4]$  (**1**) was used for this calculation to account for differences in space-group conventions.

of **1-2I<sub>2</sub>**) and a volumetric capacity of  $1.48 \text{ g cm}^{-3}$  ( $1.48 \text{ g}$  of **1-2I<sub>2</sub>** per  $1 \text{ cm}^3$  of **1-2I<sub>2</sub>**). This value is comparable to the highest gravimetric capacities reported for porous iodine storage materials of 64 and 55 wt% for Cu- and Zn-based metal–organic frameworks, respectively.<sup>[10]</sup> This nonporous material also shows a significantly higher volumetric capacity than porous frameworks. We then examined lead bromide perovskites containing alkene groups in the organic layers. The reaction of terminal alkenes with iodine typically results in reversible addition to form vicinal diiodoalkanes. In solution, the equilibrium is displaced towards the alkenes with half-lives for the diiodoalkanes of 0.075–1.2 h.<sup>[11]</sup> The alkene perovskite  $(\text{PEA})_2[\text{PbBr}_4]$  (**2**) shows an elongation of the *c* axis by 17% upon iodination to form a new layered hybrid with diiodoalkane molecules:  $(\text{PEA-I}_2)_2[\text{PbBr}_4]$  (**2-2I<sub>2</sub>**). Iodine addition across the C=C bonds is corroborated by vibrational spectroscopy that reveals a decrease in the intensity of the C=C stretch at  $1646 \text{ cm}^{-1}$  (Figure S5). Interestingly, this new phase reverts to the starting alkene material over 24 h at 25 °C (Figure S12). This expansion–contraction of the unit cell upon reaction with iodine can be repeated at least five times, even in the presence of moisture, with no loss of crystallinity (Figures S13 and S14). The half-life of the diiodoalkane hybrid can be estimated from the X-ray powder pattern to be 3.2 h at 25 °C. The solid-state structure increases the half-life of the diiodoalkane from the

solution-state value by a factor of five (compared to 1,2-diiodopentane).<sup>[11]</sup> To probe the role of the crystal structure in stabilizing the diiodoalkane, we then moved to a longer alkene. Solid  $(\text{BEA})_2[\text{PbBr}_4]$  (**3**; Figure 3a)<sup>[7]</sup> also reacts with iodine, with a 29% increase in the *c* axis, to form the iodinated material,  $(\text{BEA-I}_2)_2[\text{PbBr}_4]$  (**3-2I<sub>2</sub>**; Figure 3b). The subtle structural change in the organic molecules resulted in a significantly longer half-life of 72 h for **3-2I<sub>2</sub>**—an increase of a factor of 22 from that of **2-2I<sub>2</sub>** and of a factor of 112 from the solution-state value. The solution-state half-lives of  $\text{BEA-I}_2$  and  $\text{PEA-I}_2$  are comparable;<sup>[12]</sup> therefore, solid-state packing effects, particularly iodine–iodine interactions, are likely to stabilize the molecules. Solid-state interactions in crystals have been used to isolate metastable molecules.<sup>[13]</sup> Here, the longer molecule may accommodate a more efficient packing. In contrast,  $(\text{PEA})_2[\text{CuCl}_4]$  does not show a reaction, even upon exposure to an iodine-saturated atmosphere for four days. We attribute this to the substantially smaller Cu–Cl inorganic template compared to the Pb–Br template.<sup>[14]</sup> Stabilization of diiodoalkanes that cannot be isolated in solution and the dependence of reactivity on the size of the inorganic template support a solid–gas reaction with iodine, and is evidence against dissolution and recrystallization of the material.

Alkyne molecules react with iodine to form diiodoalkenes. However, the unique structural features of the hybrid offer significant advantages over the organic molecules alone for iodine capture. To illustrate this point, we considered the capture of radioactive iodine vapor. Nuclear power plants release radioactive iodine isotopes during the final oxidation of uranium and plutonium fission products. Iodine in cooled spent nuclear fuel consists of approximately a 3:1 isotopic ratio of  $^{129}\text{I}/^{127}\text{I}$ .<sup>[15]</sup> Whereas  $^{127}\text{I}$  is a stable isotope,  $^{129}\text{I}$  emits beta and gamma radiation with a half-life of 10 million years.<sup>[15–16]</sup> Due to its long half-life and extreme mobility in the environment  $^{129}\text{I}$  is likely to be the radionuclide with the greatest long-term environmental impact.<sup>[17]</sup> For disposal through nuclear transmutation<sup>[18]</sup> or for long-term sequestration, selective and inexpensive capture materials are required.<sup>[19]</sup> Silver-impregnated zeolites can trap iodine as silver iodide with a gravimetric capacity upper limit of ca.

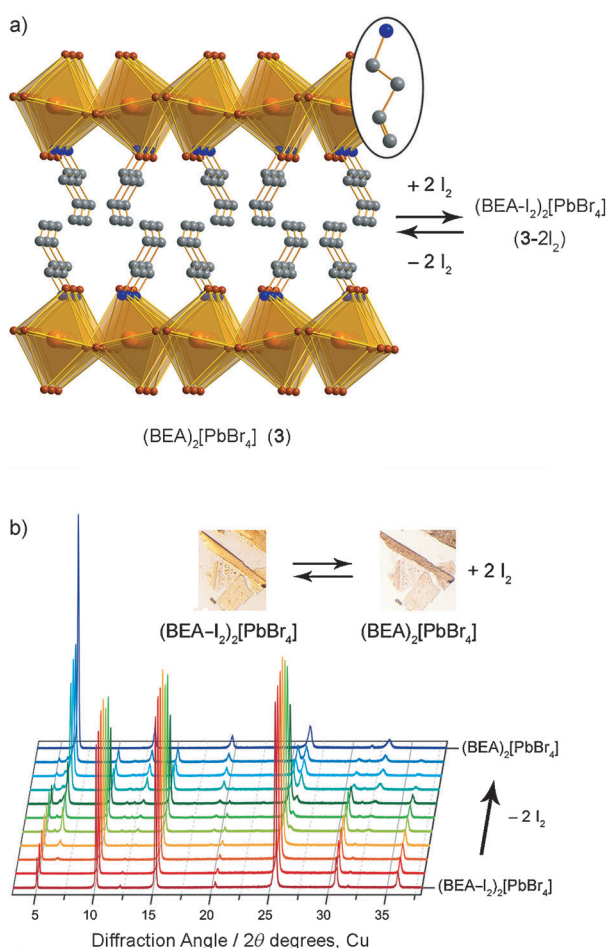


**Figure 3.** a) X-ray structure of  $(\text{BEA})_2[\text{PbBr}_4]$  (**3**). H atoms omitted for clarity. Pb Orange, Br brown, N blue, C gray. Inset shows an individual cation in the organic layers. b) Powder X-ray diffraction patterns of an oriented film of  $(\text{BEA-I}_2)_2[\text{PbBr}_4]$  (**3-2I<sub>2</sub>**) that reverts back to the diffraction pattern of **3**. The inset shows micrographs of **3-2I<sub>2</sub>** crystals before and after loss of iodine.

33 wt %.<sup>[20]</sup> However, more efficient and inexpensive capture materials are required as an essential part of nuclear energy development.<sup>[15]</sup>

These waste streams contain ca. 20–60 ppm iodine, 0.1 %  $\text{NO}_x$  gases, and high levels of water vapor.<sup>[19]</sup> We used iodine-saturated atmospheres at various temperatures to determine that **1** can capture iodine at partial pressures ranging from 39–1350 ppm (Table S1). Samples of **1** remain as crystalline solids at a relative humidity of 0–75 % at 50 °C over at least a 24 hour period (Figure S18) and is stable for months at ambient temperature and humidity. In contrast, solid (BYA)Cl deliquesces at a relative humidity as low as 11 %, and the neutral amine is a liquid. Dissolved BYA rapidly reacts with NO and  $\text{NO}_2$  to form reactive nitroalkenes that yield a variety of products.<sup>[21]</sup> Exposure of **1** to an iodine-saturated atmosphere ( $P(\text{I}_2) = 0.30$  torr, 390 ppm) containing 1 % of  $\text{NO}_2$  for 24 hours led to a decrease in iodine-capture capacity of ca. 10 % (Table S3). Capacity losses ranging from 15–65 % upon exposure to an iodine-saturated atmosphere containing  $\text{NO}_2$  have been reported for capture materials such

as zeolites, mesoporous silica, and layered-double hydroxides.<sup>[19b]</sup> The inorganic sheets also increase the thermal stability of the molecules. Thermogravimetric analyses show a mass loss at 190 °C for **1**; a temperature 50 °C higher than that of (BYA)Cl (Figure S20). The compact lead bromide sheets can also significantly attenuate the beta and gamma emissions from  $^{129}\text{I}$  compared to the organic components alone (Table S4). Our preliminary studies indicate that the alkyne hybrid could be used to capture radioactive iodine in a soft organic matrix to generate stable and compressible materials for long-term storage. Further studies must assess the binding enthalpy and capture efficiencies of the material under dynamic gas flow and with efficient gas–solid mixing.

Typically, sorbents capture gases through reversible physisorption.<sup>[1]</sup> However, chemisorption of iodine by non-porous solids to form polyiodides<sup>[22]</sup> and doped charge-transfer salts<sup>[23]</sup> have been reported. The reversible iodination of alkene molecules in hybrid perovskites is an intriguing example of gas capture through reversible chemisorption where the equilibrium for iodine release can be tuned through molecular design. Timed-release capture materials allow for inexpensive regeneration and for sustained release of substrates. Reactivity of alkene/alkyne perovskites with iodine is general to other halogens; we will report on these systems in further communications. Reversible chemisorption in non-porous sorbents allows for capture, separation, and release of substrates based on chemical reactivity and not size. These nonporous, yet responsive, hybrid materials open traditional solid-state structures to the tools of molecular synthesis.

Received: November 11, 2013

Published online: December 5, 2013

**Keywords:** chemisorption · hybrid materials · iodine · perovskite · storage

- [1] a) L. J. Murray, M. Dinca, J. R. Long, *Chem. Soc. Rev.* **2009**, 38, 1294–1314; b) S. Horike, S. Shimomura, S. Kitagawa, *Nat. Chem.* **2009**, 1, 695–704.
- [2] a) G. Mínguez Espallargas, M. Hippler, A. J. Florence, P. Fernandes, J. van de Streek, M. Brunelli, W. I. F. David, K. Shankland, L. Brammer, *J. Am. Chem. Soc.* **2007**, 129, 15606–15614; b) S. Libri, M. Mahler, G. Mínguez Espallargas, D. C. N. G. Singh, J. Soleimannejad, H. Adams, M. D. Burgard, N. P. Rath, M. Brunelli, L. Brammer, *Angew. Chem.* **2008**, 120, 1717–1721; *Angew. Chem. Int. Ed.* **2008**, 47, 1693–1697; c) C. J. Adams, H. M. Colquhoun, P. C. Crawford, M. Lusi, A. G. Orpen, *Angew. Chem.* **2007**, 119, 1142–1146; *Angew. Chem. Int. Ed.* **2007**, 46, 1124–1128.
- [3] a) J. L. Atwood, L. J. Barbour, A. Jerga, *Science* **2002**, 296, 2367–2369; b) J. L. Atwood, L. J. Barbour, A. Jerga, B. L. Schottel, *Science* **2002**, 298, 1000–1002; c) J. L. Atwood, L. J. Barbour, A. Jerga, *Angew. Chem.* **2004**, 116, 3008–3010; *Angew. Chem. Int. Ed.* **2004**, 43, 2948–2950.
- [4] a) D. B. Mitzi, *Prog. Inorg. Chem.* **1999**, 48, 1–121; b) D. B. Mitzi, C. A. Feild, W. T. A. Harrison, A. M. Guloy, *Nature* **1994**, 369, 467–469.
- [5] D. B. Mitzi, D. R. Medeiros, P. R. L. Malenfant, *Inorg. Chem.* **2002**, 41, 2134–2145.
- [6] R. J. Sundberg, F. A. Carey in *Advanced Organic Chemistry, Part B: Reactions and Synthesis*, Plenum, US, **2001**, 200–226.

- [7] CCDC 955776, 955777, 955778 contain the supplementary crystallographic data for this paper. These data can be obtained free of charge from The Cambridge Crystallographic Data Centre via [www.ccdc.cam.ac.uk/data\\_request/cif](http://www.ccdc.cam.ac.uk/data_request/cif).
- [8] *Mercury CSD 3.1* Cambridge Crystallographic Data Centre, **2012**.
- [9] I. Halasz, *Cryst. Growth Des.* **2010**, *10*, 2817–2823.
- [10] a) D. F. Sava, K. W. Chapman, M. A. Rodriguez, J. A. Greathouse, P. S. Crozier, H. Zhao, P. J. Chupas, T. M. Nenoff, *Chem. Mater.* **2013**, *25*, 2591–2596; b) D. F. Sava, M. A. Rodriguez, K. W. Chapman, P. J. Chupas, J. A. Greathouse, P. S. Crozier, T. M. Nenoff, *J. Am. Chem. Soc.* **2011**, *133*, 12398–12401. The reported capacities were recalculated as wt% = mass of iodine/[(mass of iodine)+(mass of capture material)] for ease of comparison.
- [11] K. W. Field, D. Wilder, A. Utz, K. E. Kolb, *J. Chem. Educ.* **1987**, *64*, 269–271.
- [12] P. W. Robertson, J. B. Butchers, R. A. Durham, W. B. Healy, J. K. Heyes, J. K. Johannesson, D. A. Tait, *J. Chem. Soc.* **1950**, 2191–2194.
- [13] B. Kahr, R. W. Gurney, *Chem. Rev.* **2001**, *101*, 893–952.
- [14] D. B. Mitzi, *J. Chem. Soc. Dalton Trans.* **2001**, 1–12.
- [15] D. R. Haefner, T. J. Tranter, Methods of gas phase capture of iodine from fuel reprocessing off-gas: A literature survey, Idaho National Laboratory, Idaho Falls, ID, **2007**.
- [16] D. Strominger, J. Hollander, G. Seaborg, *Rev. Mod. Phys.* **1958**, *30*, 585–904.
- [17] G. Snyder, U. Fehn, *Nucl. Instrum. Methods Phys. Res. Sect. B* **2004**, *223–224*, 579–586.
- [18] C. D. Bowman, et al., *Nucl. Instrum. Methods Phys. Res. Sect. A* **1992**, *320*, 336–367.
- [19] a) D. R. Haefner, J. Law, T. J. Tranter, System design description and requirements for modeling the off-gas systems for fuel recycling facilities, Idaho National Laboratory, Idaho Falls, ID, **2010**; b) Y. Wang, et al., Development of a New Generation of Waste Form for Entrapment and Immobilization of Highly Volatile and Soluble Radionuclides, Sandia National Laboratories, **2010**.
- [20] a) B. R. Westphal, D. G. Cummings, J. J. Giglio, D. L. Wahlquist, K. J. Bateman, W. M. McCartin, J. J. Park, J. M. Shin, B. D. Begg, *Mater. Res. Soc. Symp. Proc.* **2010**, *1265*, AA02–04; b) K. W. Chapman, P. J. Chupas, T. M. Nenoff, *J. Am. Chem. Soc.* **2010**, *132*, 8897–8899.
- [21] B. R. Brown, *The Organic Chemistry of Aliphatic Nitrogen Compounds*, Oxford University Press, Oxford, **1994**, pp. 470–484.
- [22] L. Mohanambe, S. Vasudevan, *Inorg. Chem.* **2004**, *43*, 6421–6425.
- [23] A. Funabiki, T. Mochida, K. Takahashi, H. Mori, T. Sakurai, H. Ohta, M. Uruichi, *J. Mater. Chem.* **2012**, *22*, 8361–8366.